

Comparative Studies of Rare-Earth Element Y-Doped In_2O_3 by First-Principles Calculations *

BAI Li-Na(白丽娜)^{1,2}, FENG Li-Feng(冯立峰)², WANG Rui(王睿)¹,
JIANG Qing(蒋青)¹, LIAN Jian-She(连建设)^{1**}

¹The Key Lab of Automobile Materials (Ministry of Education), College of Materials Science and Engineering,
Jilin University, Changchun 130025

²The Key Laboratory of Photonic and Electric Bandgap Materials (Ministry of Education),
School of Physics and Electronic Engineering, Harbin Normal University, Harbin 150025

(Received 16 December 2013)

In_2O_3 doped with rare-earth element yttrium shows improved optoelectronic efficiency. Here the structural properties and electronic structures of Y-doped In_2O_3 are investigated by using a first-principles approximation. For $\text{In}_{1.9375}\text{Y}_{0.0625}\text{O}_3$, the d site is the more stable site. The Y_i^{3+} interstitial has a low formation energy and is a possible interstitial defect, which would lead to shallow and abundant donors without sacrificing optical transparency. Since defects are universally distributed in In_2O_3 or doped In_2O_3 , complex defect configurations are also calculated.

PACS: 71.15.Mb, 71.20.-b, 71.20.Nr

DOI: 10.1088/0256-307X/31/8/087101

Transparent conducting oxides (TCOs) exhibit the attractive properties of high metallic conductivity and insulator-like transparency in the visible range. In_2O_3 is a prototypical n-type TCO.^[1] Recently, indium oxide thin films doped with cycle-V elements have been investigated.^[2–5] Simultaneously, high mobility has been obtained by doping rare earth elements such as Y in In_2O_3 thin films.^[6] However, the related mechanism is unclear.

To further enhance the mobility and hence to increase the electrical conductivity of In_2O_3 , without sacrificing its optical transparency, it is helpful to investigate the electronic structures and optical properties of metal or rare earth elements doped In_2O_3 . In this Letter, the potential advantages of Y-doped In_2O_3 are theoretically investigated by using a first-principles approximation, where the calculated electronic and optical properties are compared to those of commercial $\text{In}_2\text{O}_3\text{:Sn}$ (ITO). The results suggest that doping of Y into appropriate In_2O_3 lattice sites could achieve a significant blue-shift in the energy gap and induce high mobility to increase the electrical conductivity, without sacrificing its optical transparency.

In_2O_3 crystal has a cubic bixbyite structure with a space group of $Ia-3$, as shown in Fig. 1. The indium atoms are located at two non-equivalent six-fold coordinated sites, which are referred to as $8b$ and $24d$ sites, and the O atoms occupy the $48e$ site. Simultaneously, the crystal contains two vacancies, i.e. a and c sites, corresponding to the 3 and 4 sites in Fig. 1. Y_2O_3 also has the same structure. To describe the config-

uration of Y doping in the In_2O_3 lattice, some possible models of $\text{In}_{1.9375}\text{Y}_{0.0625}\text{O}_3$, $\text{In}_{1.875}\text{Y}_{0.125}\text{O}_3$, and $\text{In}_2\text{Y}_{0.0625}\text{O}_3$ (Y_i) are designed, and the complex configurations of defect pair ($\text{Y}_i\text{-Y}_{\text{In}}$, $\text{Y}_i\text{-V}_{\text{In}}$, and $\text{Y}_i\text{-V}_{\text{O}}$) are used, where Y_{In} , Y_i , V_{In} , and V_{O} are Y substituting In, Y interstitial and In atom or O atom vacancies, respectively.

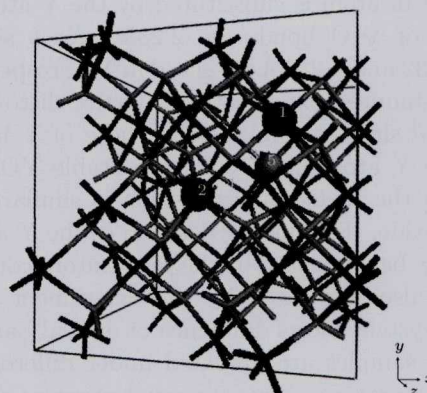


Fig. 1. The structure of bixbyite In_2O_3 is depicted in a ball and stick representation (the 1 site of the In atom at site b , the 2 site of the In atom at site d , the 3 to 4 of the possible interstitial sites a and c , and the 5 site of the O atom).

The theoretical calculations are performed on the Cambridge serial total energy package (CASTEP) code. The exchange and correlation effects are described by the local density approximation (LDA).^[7,8] A plane wave cutoff of 500 eV and a $3 \times 3 \times 3$ k -point mesh are found to reach sufficient convergence. The

*Supported by the National Natural Science Foundation of China under Grant Nos 50871046 and 11247271, the National Basic Research Program of China under Grant No 2010CB631001, the Programs of Education Bureau of Heilongjiang Province under Grant No 12531210, and the Program for Changjiang Scholars and Innovative Research Team in University.

**Corresponding author. Email: lianjs@jlu.edu.cn

© 2014 Chinese Physical Society and IOP Publishing Ltd

formation energy is calculated to examine the relative stability on the charge state q .^[9–11] The chemical potentials depend on the experimental growth conditions, which can be either In-rich or O-rich, and the sources of Y are yttrium oxide. The calculated formation energies ΔH_f (In_2O_3) (-11.069 eV) and ΔH_f (Y_2O_3) (-21.297 eV) are slightly larger than the experimental values (-9.63 eV and -19.41 eV).^[12,13] Simultaneously, yttrium substituting on the In site presents the same valence states, we therefore only study the neutral charge state of Y_{In}^0 ($q = 0$). For the Y interstitial, charge states from treble charge state Y_i^{3+} ($q = +3$) to neutral charge state Y_i^0 ($q = 0$) are considered.

For the substitution structures of Y-doped In_2O_3 , the environment indium atoms are distorted. As the

ionic radius of Y^{3+} (0.89 \AA) is slightly larger than that of In^{3+} (0.81 \AA), the replacement of In by Y should cause a lattice expansion,^[6] in the case of d -site substitution (Y_{In}), lattice constant c increases from 10.154 \AA for In_2O_3 to 10.185 \AA . To compare the relative stability, the formation energies of various configurations are calculated, and summarized in Table 1. For the substitution configuration of Y_{In} , the formation energies of the b site and d site are similar, which are lower than those of the interstice and coexistence configurations in the neutral charge state, and the d site has the smallest formation energy, thus site d is the energy stable site. This result is different from the Sn-doped In_2O_3 configuration, where site b is the most preference site.^[14–17]

Table 1. Formation energies of various doping sites of Y-doped In_2O_3 . Values are given for the limiting chemical potentials of In-rich conditions, and for $E_F = 0$, i.e., E_F located at the top of the valence band.

In-rich	Y_{In}		Y_i				$\text{Y}_i\text{-Y}_{\text{In}}$		$\text{Y}_i\text{-V}_{\text{In}}$		$\text{Y}_i\text{-V}_\text{O}$
	b site	d site	Y_i^0	Y_i^{1+}	Y_i^{2+}	Y_i^{3+}	b site	d site	b site	d site	
Formation energies (eV)	0.38	0.28	3.88	1.03	-1.29	-2.99	6.05	5.43	4.65	4.56	5.33

The chemical bond characteristic is calculated after geometry optimization. For the pure- In_2O_3 system, the distances of In-O bonds are 2.182 \AA for the b site and 2.135 , 2.202 and 2.229 \AA for the d sites.^[14] When the In atom is substituted by the Y atom, the distances of Y-O bonds are 2.238 \AA for b site and 2.192 , 2.232 and 2.288 \AA for site d in Y_{In} , respectively. Thus the induced expansion and lattice distortion of Y in the d site are smaller than those of Y in the b site. The Y atom likes to form a stable YO_6 octahedron in the In_2O_3 lattice, which is similar to the yttrium oxide. The doping position of the Y atom in In_2O_3 may be influenced by the preparatory condition, which is also motivated by the experiment finding that the system shows difference of optical band gap, when the samples are prepared under different substrate temperatures, oxygen partial pressure and film thickness.^[18–20] Simultaneously, doping the Y atom induces distortion in the adjacent InO_6 octahedron of atoms. The correlation between the photocatalytic activity and a distorted oxygen-metal octahedron has been demonstrated in a series of p-block metal oxide photocatalysts.^[21] The distorted unsymmetrical fields would promote electron-hole separation,^[22–25] thus Y-doping may improve the photoelectric activity of In_2O_3 .

The band structures with four high symmetry lines $X(1/2, 0, 0)\text{-}R(1/2, 1/2, 1/2)\text{-}M(1/2, 1/2, 0)\text{-}G(0, 0, 0)\text{-}R(1/2, 1/2, 1/2)$ and partial density of states (PDOS) are shown in Fig. 2. The calculated band gap of In_2O_3 (1.010 eV) is much smaller than the experimental optical band gap (2.619 eV).^[26] However, we focus on the relative change between undoped and

doped systems, thus the variation of the band gap value is the concern. Clearly, the Y atom doping significantly affects the band structure. The d site doping of Y_{In} induces an increase or blue shift of the band gap, the obtained values of 1.084 and 1.097 eV for an indirect band gap (E_g^{ind}) and direct band gap (E_g^{dir}) are shown in Fig. 2(b). The band structure of $\text{In}_{1.875}\text{Y}_{0.125}\text{O}_3$ also shows the blue shift of the band gap from 1.010 eV for In_2O_3 to 1.196 eV , the obtained values of 1.196 and 1.225 eV for indirect band gap (E_g^{ind}) and direct band gap (E_g^{dir}) are shown in Fig. 2(c). Due to the fact that the band gap of Y_2O_3 is much larger than that of In_2O_3 , thus a small proportion of Y doping, can evidently increase the band gap. Compared with the band structure of In_2O_3 , the flat topmost valence band (VB) and high dispersion conduction band (CB) are retained. Doping of Y also induces the splits in VB and CB due to breaking the symmetry of the In_2O_3 lattice, similar to the case of an Sn-doped In_2O_3 lattice.^[14] However, in contrast to the Sn-doped In_2O_3 lattice, the d^1 electron of the Y atom is more sensitive to the surrounding oxygen than the spherically symmetric s -electron of the Sn atom, thus the d^1 electron participates in bonding and appears in the highest valence band.

Here we present the calculated results of absorption spectra in the wavelength range from 200 nm to 600 nm with light polarized perpendicular to the c axis ($E \perp c$), as shown in Fig. 3. Due to the underestimation of the LDA approach on the band gap and the delay of the optical absorption,^[14,26,27] the calculated absorption onset is much smaller than the experimental value. Thus the scissors operator approach with a

value of 1.60 eV is used to fit the absorption edge to the experimental value. For the absorption spectra of pure In_2O_3 , the computational absorption edge is consistent with the previous theoretical and experimental results.^[26,28–30] Compared with In_2O_3 , the d^{10} -shell In ion is substituted by the d^1 -shell Y ion in Y_{In} , which will cause the lifting of CB and the increasing of the band gap. Thus it is believed that the blue shift of the optical absorption will improve the optical transparency in the visible region. The absorption spectra of Sn-doped In_2O_3 are presented in Fig. 3. It is seen that, in consideration of the absorption onset, the Sn-doped In_2O_3 has better optical transparency than the Y-doped In_2O_3 due to the BM shift.^[14]

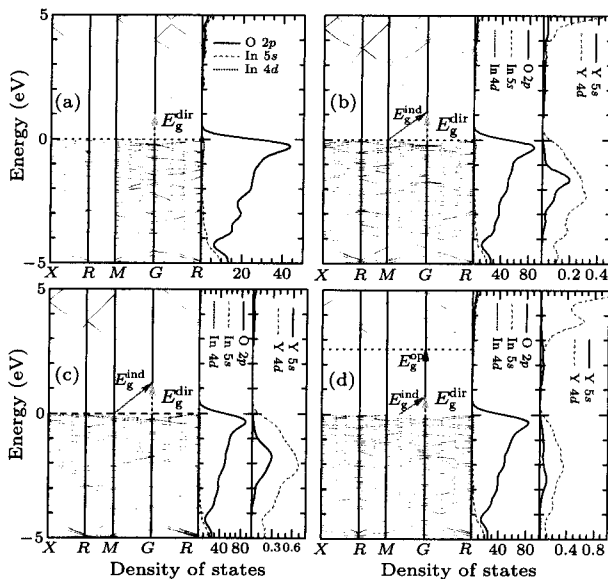


Fig. 2. Band structures and density of states of (a) In_2O_3 , (b) $\text{In}_{1.9375}\text{Y}_{0.0625}\text{O}_3$, (c) $\text{In}_{1.875}\text{Y}_{0.125}\text{O}_3$, and (d) $\text{In}_2\text{Y}_{0.0625}\text{O}_3$. The red, green, black-directed lines represent the indirect band gap (E_g^{ind}), direct band gap (E_g^{dir}), and optical band gap (E_g^{opt}). The band energies are referenced to the top of the In_2O_3 valence band. The Fermi levels at 0 eV, 0 eV, 0 eV and 2.624 eV, respectively, are indicated by a horizontal dotted line.

The on-site Coulomb interaction parameter U is introduced in the LDA approach to improve the prediction of the band gap.^[14] Here the parameter U is introduced on In-4d, Y-4d and O-2p orbits. The calculated direct band gap of In_2O_3 is 2.591 eV, which is closer to the experimental value of 2.619 eV; and that of $\text{In}_{1.875}\text{Y}_{0.125}\text{O}_3$ (6.25 at% Y doping) is 2.798 eV of the indirect band gap.

For the Y interstitial, charge states of Y_i^0 to Y_i^{3+} are considered. Two models are selected that the Y atoms respectively occupy a or c sites. The calculation results show that the Y atom in the c site is the preferred site. Accordingly, the structure feature of the Y atom in the c site for interstitial configurations will be discussed in the following.

The formation energies for four charge states of Y_i

are also listed in Table 1. Under the In-rich condition, the formation energies of Y_i^0 to Y_i^{3+} are 3.88 eV to -2.99 eV, respectively. Hence, the Y_i defect will lead to abundant donor states with a stable 3+ charge state. We investigate the structural changes in the lattice. The local structures for the charge states of Y_i^0 and Y_i^{3+} are schematically illustrated in Fig. 4. For Y_i^{3+} doping, the Y-O bond lengths (between Y and the six nearest-neighbor O atoms) relax inward by 4.8% in comparison with the Y-O bond lengths of Y_i^0 . The charge-neutral Y atom (covalent radius of 1.62 Å) placed in the interstitial site c causes the bond angle distortion and high formation energy. On the other hand, the Y_i^{3+} ion (ionic radius of 0.89 Å) is small enough to fit the space around the interstitial site c . Thus the contraction of the Y-O bond length is expected. The defect transition energy $\epsilon(3+/0)$ of Y_i^{3+} is found at 0.326 eV below the bottom of the conduction band (CBM) with extrapolation to the results for the experimental band gap (2.619 eV) under the In-rich limit. However, due to the low formation energy and the defect transition energy, it is possible that the Y_i^{3+} defect or similar defects exist in Y doped In_2O_3 during the prepared process, which turns the samples to have an n-type conductivity. We can conclude that the Y_i defect permits the generation of photoexcited electrons at the conduction bands.

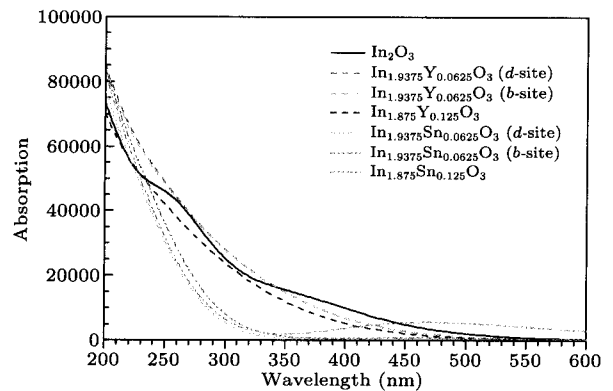


Fig. 3. The absorption spectra of In_2O_3 , b -site substitution and d -site substitution for $\text{In}_{1.9375}\text{X}_{0.0625}\text{O}_3$, and $\text{In}_{1.875}\text{X}_{0.125}\text{O}_3$ ($X = \text{Y}$ or Sn) in the UV and visible light spectrum with absorption polarized perpendicular to the c axis.

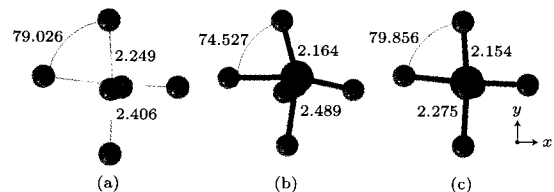


Fig. 4. Schematic representation of the local structure O octahedral of (a) In_2O_3 , (b) Y_i^0 , and (c) Y_i^{3+} , respectively. Red spheres represent O atoms and green spheres represent Y atoms.

The electronic structure of Y_i^0 is shown in Fig. 2(d),

near CBM, some new impurity bands of Y 5s state have been introduced. The presence of impurity bands can absorb low-energy photons which can excite electrons from the valence bands to the intermediate bands, where most possible electron transitions are marked with green dashes, which is the electronic transition between the O 2p state in the highest valence band and the 5s state of metal atoms in the impurity band. Later they can be excited to above CBM for effective photovoltaic energy conversion. Therefore, the defect structure may play an important role, as the impurity bands permit enhanced carrier separation, so mobile electrons of various energetic states within them can offer enhanced electron conductivity. Especially for the conduction band, the pronounced Burstein–Moss (BM) shift, the abruptions of intermediate bands and conduction bands ensure optical transparency, which is vital for device performance.^[31]

Since interstitial Y is a donor, we expect that it will constraint with substitutional Y and the intrinsic defect. Thus we also study complex defect configurations of the Y_i – Y_{In} , Y_i – V_{In} , and Y_i – V_O . Different defect pairs are obtained by substituting or removing the interstitial atom near the neutral metal or oxygen atom. The high formation energy of Y_i – Y_{In} from large electrostatic repulsion between the doped atoms due to the ionic radius of Y^{3+} (0.89 Å) is larger than that of In^{3+} (0.81 Å). The result implies that the defect pair of Y_i – Y_{In} cannot exist, thus the cluster of metal atoms is negligible in the crystal. Surprisingly, the existence of Y_i – V_{In} is found to relax to the Y_{In} defect with high formation energy. The most prominent intrinsic electron killer (acceptor) is the cation site vacancy V_{In} , thus the Y-doping profitably obtains n-type conductivity. Similar to the above results, the Y_i – V_O configuration also has high formation energy, and this suggests an unfavorable role.

In summary, our calculations of rare-earth element Y doped In_2O_3 provide detailed information on the structural, electronic and optical properties. We find that substitutional Y_{In} of the *d* site is more stable, and will lead to the blue shift of the optical band gap. The Y_i is a treble donor with lower formation energy and defect transition energy. It is likely that Y_i emerges during growth, and photo-excited electrons which are subsequently generated have high mobility at the conduction bands without sacrificing optical transparency. Our calculations also show that the defect pair of Y_i – Y_{In} cannot exist, thus the cluster of metal atoms is negligible in the crystal. The metastable defect pair of Y_i – V_{In} will lead to the formation of the Y_{In} defect when enough fluctuations in

energy are provided.

References

- [1] Tomita T, Yamashita K, Hayafuji Y and Adachi H 2005 *Appl. Phys. Lett.* **87** 051911
- [2] Zhang J, Qing X, Jiang F H and Dai Z H 2003 *Chem. Phys. Lett.* **371** 311
- [3] Meng Y, Yang X L, Chen H X, Shen J, Jiang Y M, Zhang Z J and Hua Z Y 2001 *Thin Solid Films* **394** 218
- [4] Warmingsingh C, Yoshida Y, Readey D W, Teplin C W, Perkins J D, Parilla P A, Gedvilas L M, Keyes B M and Ginley D S 2004 *J. Appl. Phys.* **95** 3831
- [5] Medvedeva J E 2006 *Phys. Rev. Lett.* **97** 086401
- [6] Arai N, Saito N, Nishiyama H, Shimodaira Y, Kobayashi H, Inoue Y and Sato K 2008 *J. Phys. Chem. C* **112** 5000
- [7] Hohenberg P and Kohn W 1964 *Phys. Rev.* **136** B864
- [8] Kohn W and Sham L J 1965 *Phys. Rev.* **140** A1133
- [9] Van de Walle C G, Limpijumnong S and Neugebauer Jörg 2001 *Phys. Rev. B* **63** 245205
- [10] Limpijumnong S, Zhang S B, Wei S H and Park C H 2004 *Phys. Rev. Lett.* **92** 155504
- [11] Kihç Ç and Zunger A 2002 *Phys. Rev. Lett.* **88** 095501
- [12] Reunchan P, Zhou X, Limpijumnong S, Janotti A and Van de Walle C G 2011 *Curr. Appl. Phys.* **11** S296
- [13] Zheng J X, Ceder G, Maxisch T, Chim W K and Choi W K 2006 *Phys. Rev. B* **73** 104101
- [14] Bai L N, Wei Y P, Lian J S and Jiang Q 2013 *J. Phys. Chem. Solids* **74** 446
- [15] Skoulidis N and Polatoglou H M 2007 *Thin Solid Films* **515** 8728
- [16] Brewer S H and Franzen S 2004 *Chem. Phys.* **300** 285
- [17] Kompany A, Aliabad H A R, Hosseini S M and Baedi J 2007 *Phys. Stat. Sol. B* **244** 619
- [18] Wei H L, Zhang L, Liu Z L and Yao K L 2011 *Chin. Phys. B* **20** 118102
- [19] Sun S H, Wu P and Xing P F 2013 *Chin. Phys. Lett.* **30** 077503
- [20] Öztas M, Bedir M, Öztürk Z, Korkmaz D and Sur S 2006 *Chin. Phys. Lett.* **23** 1610
- [21] Sato J, Kobayashi H and Inoue Y 2003 *J. Phys. Chem. B* **107** 7970
- [22] Inoue Y, Asai Y and Sato K 1994 *J. Chem. Soc.-Faraday Trans.* **90** 797
- [23] Kohno M, Ogura S, Sato K and Inoue Y 1997 *Chem. Phys. Lett.* **267** 72
- [24] Inoue Y, Kubokawa T and Sato K 1991 *J. Phys. Chem.* **95** 4059
- [25] Ogura S, Kohno M, Sato K and Inoue Y 1999 *Phys. Chem. Chem. Phys.* **1** 179
- [26] Walsh A, Da Silva J L F, Wei S H, Körber C, Klein A, Piper L F J, DeMasi A, Smith K E, Panaccione G, Torelli P, Payne D J, Bourlange A and Egdell R G 2008 *Phys. Rev. Lett.* **100** 167402
- [27] Bai L N, Sun H M, Lian J S and Jiang Q 2012 *Chin. Phys. Lett.* **29** 117101
- [28] King P D C, Veal T D, Fuchs F, Wang Y, Payne D J, Bourlange A, Zhang H, Bell G R, Cimalla V, Ambacher O, Egdell R G, Bechstedt F and McConville C F 2009 *Phys. Rev. B* **79** 205211
- [29] Hamberg I and Granqvist C G 1986 *J. Appl. Phys.* **60** R123
- [30] Weiher R L and Ley R P 1966 *J. Appl. Phys.* **37** 299
- [31] Burbano M, Scanlon D O and Watson G W 2011 *J. Am. Chem. Soc.* **133** 15065